Kinetics of Proton Uptake and Dye Binding by Photoactive Yellow Protein in Wild Type and in the E46Q and E46A Mutants†

Berthold Borucki,‡ Savitha Devanathan,§ Harald Otto,‡ Michael A. Cusanovich,§ Gordon Tollin,§ and Maarten P. Heyn*,‡

Biophysics Group, Department of Physics, Freie Universität Berlin, Arnimallee 14, D-14195 Berlin, Germany, and Department of Biochemistry and Molecular Biophysics, University of Arizona, Tucson, Arizona 85721

Received February 4, 2002; Revised Manuscript Received May 2, 2002

ABSTRACT: We studied the kinetics of proton uptake and release by photoactive yellow protein (PYP) from *Ectothiorhodospira halophila* in wild type and the E46Q and E46A mutants by transient absorption spectroscopy with the pH-indicator dyes bromocresol purple or cresol red in unbuffered solution. In parallel, we investigated the kinetics of chromophore protonation as monitored by the rise and decay of the blue-shifted state I_2 ($\lambda_{max} = 355$ nm). For wild type the proton uptake kinetics is synchronized with the fast phase of I_2 formation ($\tau = 500$ μs at pH 6.2). The transient absorption signal from the dye also contains a slower component which is not due to dye deprotonation but is caused by dye binding to a hydrophobic patch that is transiently exposed in the structurally changed and partially unfolded I_2 intermediate. This conclusion is based on the wavelength, pH, and concentration dependence of the dye signal and on dye measurements in the presence of buffer. SVD analysis, moreover, indicates the presence of two components in the dye signal: protonation and dye binding. The dye binding has a rise time of about 4 ms and is coupled kinetically with a transition between two I_2 intermediates. In the mutant E46Q, which lacks the putative internal proton donor E46, the formation of I_2 is accelerated, but the proton uptake kinetics remains kinetically coupled to the fast phase of I_2 formation ($\tau = 100$ μs at pH 6.3). For this mutant the protein conformational change, as monitored by the dye binding, occurs with about the same time constant as in wild type but with reduced amplitude. In the alkaline form of the mutant E46A the formation of the I_2-like intermediate is even faster as is the proton uptake ($\tau = 20$ μs at pH 8.3). No dye binding occurred in E46A, suggesting the absence of a conformational change. In all of the systems proton release is synchronized with the decay of I_2. Our results support mechanisms in which the chromophore of PYP is protonated directly from the external medium rather than by the internal donor E46.

Photoactive yellow protein (PYP)[1] from the purple bacterium *Ectothiorhodospira halophila* (*1*) is a small water-soluble photoreceptor that is believed to be involved in negative phototaxis (*2*). PYP has recently attracted further attention as the structural prototype for the PAS and LOV domains of a large class of receptor proteins (*3*). Its blue light absorption ($\lambda_{max} = 446$ nm) is due to a thioester-linked *p*-hydroxycinnamoyl chromophore. In the dark state P, the anionic form of the chromophore (*4*), is stabilized by hydrogen bonds to E46 and Y42 (*5*, *6*), and the 7−8 double bond of the chromophore is trans. Photoexcitation is followed by rapid isomerization around this bond (*7*, *8*) and a photocycle consisting of a number of spectrally distinguishable photointermediates (*9*, *10*). We will use the nomenclature of ref *11* to designate these intermediates. About 3 ns after photoexcitation the red-shifted intermediate I_1 is formed ($\lambda_{max} = 465$ nm, $\tau \approx 200$ μs) in which the hydrogen bond with E46 is still intact (*12*, *13*). In the following long-lived blue-shifted intermediate I_2 ($\lambda_{max} = 355$ nm, $\tau \approx 200$ ms), this hydrogen bond is broken, and the phenolate moiety has rotated out of its initial binding pocket, exposing its oxygen to the solvent (*14*). In I_2 the cis form of the chromophore is protonated (*8*, *15*), leading to the large spectral blue shift. The source of the proton that protonates the chromophore remains unclear and is the focus of the present study. The long-lived I_2 intermediate is presumed to be the signaling state. Evidence from X-ray diffraction, NMR, and FTIR indicates that during the formation of I_2 (or between two sequential I_2 states) a major global structural change occurs which has been described as a partial unfolding (*14*, *16*−*18*). In I_2 a hydrophobic surface patch is exposed which may be involved in signal transduction (*19*). Results from NMR and FTIR also indicate that the structural changes observed for I_2 in solution are much larger than those observed by X-ray diffraction with crystals (*17*, *18*). The receptor returns from I_2 in about 200 ms to the initial P state. In this final

† This work was supported in part by Grant Sfb 498-TP B1 from the Deutsche Forschungs Gemeinschaft to M.P.H. and NSF Grant MCB-97227181 to M.A.C.

* To whom correspondence should be addressed. E-mail: heyn@physik.fu-berlin.de. Fax: 49-30-8385 6299. Phone: 49-30-8385 6141.

‡ Freie Universität Berlin.

§ University of Arizona.

[1] Abbreviations: PYP, photoactive yellow protein; FTIR, Fourier transform infrared; SVD, singular value decomposition; BCP, bromocresol purple; CR, cresol red; BSA, bovine serum albumin; PAS, acronym formed from the names of the first three proteins (*p*eriod clock protein of *Drosophila*, *a*ryl hydrocarbon receptor nuclear translocator of vertebrates, *s*ingle-minded protein of *Drosophila*) recognized as sharing this sensory motif; LOV, *l*ight, *o*xygen, and *v*oltage.

10.1021/bi0256227 CCC: $22.00
Published on Web 07/13/2002

transition the chromophore reisomerizes and deprotonates, and the structural change is reversed. The structural changes of PYP were also detected by nanosecond time-resolved X-ray diffraction at room temperature (*20*).

It was recently suggested using time-resolved FTIR that there are two sequential I_2 intermediates, both with a protonated chromophore and a deprotonated E46 carboxyl group (*21*). In the transition from I_1 to I_2' (rise time about 260 μs at room temperature and pH 7), the carboxyl group of E46 deprotonates, and the chromophore protonates (*21*). In this state only local structural changes have occurred around the chromophore. In the following step from I_2' to I_2 (2 ms), large changes in the secondary structure occur as monitored by changes in the amide I band (*21*). According to these authors the protonation changes are followed by the large global conformational change with considerable delay (260 μs/2 ms). Similar FTIR experiments were performed by another group that reached somewhat different conclusions and employed a different photocycle model (*13*). They interpreted their data in terms of branching after I_1. In the faster step ($\tau = 113$ μs) E46 moves into a more hydrophobic environment but stays protonated in a fraction of the molecules (i.e., a I_1' state), whereas in the majority of the molecules E46 deprotonates (I_2) (*13*). In the slower phase ($\tau = 1.5$ ms) further deprotonation of E46 from the molecules in I_1' occurs as well as a significant change in the protein backbone (*13*). The processes of E46 deprotonation, chromophore protonation, and secondary structure changes all occur with both time constants of 113 μs and 1.5 ms in ref *13*, whereas in ref *21* the protonation changes are associated with the faster time and the structural changes with the slower time.

Using the pH-indicator dye bromocresol purple it was shown that at pH 6.3 formation and decay of I_2 are associated with proton uptake and release, respectively, from the aqueous medium (*22*, *23*). Due to its charge and hydrogen-bonding interactions with E46 and Y42, the chromophore has a very low p*K* of 2.8 in the dark. These interactions are lost after chromophore isomerization and rotation, leading to a large increase in its p*K*. Since the phenolate oxygen becomes exposed to the solvent in I_2 (*14*), these dye experiments suggested that the chromophore is protonated directly from the external medium (*14*). Time-resolved FTIR measurements indicated that the carboxyl group of E46 deprotonates during the formation of I_2 concurrently with the protonation of the chromophore (*13*, *21*). On the basis of this evidence these authors suggested that the chromophore is protonated intramolecularly from E46 (*13*, *21*), thereby implying that in its subsequent rotation to the protein surface the chromophore is already protonated. It is currently unclear what the source of the protons is that leads to chromophore protonation. This is the question addressed in this paper.

Protonation/deprotonation reactions of the chromophore and apoprotein are of great significance in the formation of the active signaling state of a number of photoreceptors such as rhodopsin (*24*−*26*), sensory rhodopsin (*27*), and phytochrome (*28*, *29*), as well as for the light-driven proton pump bacteriorhodopsin (*30*, *31*). This provides further motivation to investigate the mechanism of chromophore protonation and H^+ uptake in PYP. We used time-resolved flash spectroscopy to monitor the kinetics of formation and decay of the protonated chromophore (blue-shifted I_2 intermediate). To time-resolve the kinetics of proton uptake and release, we employed the pH-indicator dyes bromocresol purple (p*K* 6.3) and cresol red (p*K* 8.3). For wild type we confirm the previous findings of a tight kinetic coupling between I_2 formation/decay and H^+ uptake/release from the aqueous medium, respectively (*22*). We find, moreover, that the absorption signal at 370 nm associated with the I_2 intermediate contains two time constants around 1 ms, both of which are also contained in the dye signal. The faster component ($\tau = 500$ μs) represents the proton uptake, and the slower component ($\tau = 4$ ms) is due to transient dye binding to the changed surface structure in I_2. Similar experiments were performed with the mutant E46Q in which a hydrogen bond between Q46 and the chromophore can still form but in which no proton transfer can occur between these groups. In E46Q the rise of I_2 and the H^+ uptake are considerably accelerated with respect to wild type but remain synchronized. Further experiments were carried out with the mutant E46A, in which no H-bond between A46 and the chromophore exists and no proton transfer between these groups can occur. In this mutant formation of I_2 is even faster as is H^+ uptake. We conclude that the chromophore is most likely protonated from the external medium rather than internally from E 46.

MATERIALS AND METHODS

Sample Preparation. Native PYP from *E. halophila* and the mutants E46Q and E46A were prepared as described (*6*, *32*). Buffer removal was performed by size-exclusion chromatography on Sephadex G-25 fine (Pharmacia).

Transient Absorption Spectroscopy. Absorbance changes of unbuffered solutions of PYP were recorded after laser flash excitation from ~100 ns to 20 s. A laboratory-built apparatus was used which has previously been described in detail (*33*). From this setup the polarizing and depolarizing elements have been removed; i.e., the excitation was only from one direction, and the measuring beam was unpolarized. For the excitation in the main absorption band of PYP the laser dyes stilbene 3 dissolved in methanol (emission maximum at ~430 nm) and coumarin 47 dissolved in propylene carbonate (emission maximum at ~440 nm) were used. The output power of the dye laser was up to 5 mJ, and the pulse length was about 10 ns. The samples were measured at a minimum of three characteristic wavelengths. To detect protonation changes in the external medium, the pH-indicator dye bromocresol purple or cresol red was added to the protein solution. The absorption maximum of the deprotonated form is 590 nm for bromocresol purple ($pK_a = 6.2$) and 570 nm for cresol red ($pK_a = 8.2$). The absorbance changes were measured at a number of wavelengths over the absorption band of the deprotonated dye species. For wavelengths above 520 nm these signals reflect the dye kinetics and do not include contributions from the protein. The dye signal was also measured at the same wavelengths after addition of buffer (10 mM sodium phosphate at pH 6.2 and 10 mM Tris at pH 8.3, respectively). All measurements were performed at room temperature.

Protonation Stoichiometry. The number of protons per cycling PYP was determined by a new method which is based on the assumption that the protein and the dye act as competing buffers. At low dye concentration the protein

dominates the buffering and the signal scales with the dye concentration, while at high dye concentration the buffering effect of the protein is negligible. This suggests a saturation curve of the dye signal as a function of the dye concentration. The quantitative relationship (a derivation is given in the appendix) is

$$\Delta A(f) = \Delta A(1)\frac{f}{1 + (f - 1)/p} \qquad (1)$$

with f the relative dye concentration, $\Delta A(1)$ the dye signal at the reference dye concentration $f = 1$, and the parameter p the ratio $\Delta A(f \rightarrow \infty)/\Delta A(1)$. To determine the parameters $\Delta A(1)$ and p, the dye signal was measured at the dye concentrations 10, 20, 30, and 40 μM, and the data were fitted to eq 1. From the depletion signal (the bleach of the dark state P) the fraction of cycling molecules was estimated. This requires a correction of the measured depletion signal for the contribution of the dye at the measuring wavelength λ:

$$\Delta A_{corr}(\lambda,t) = \Delta A_{meas}(\lambda,t) + \Delta A_{dye}(\lambda_{dye},t)x \qquad (2)$$

The factor $x = \Delta A_{dye}(\lambda)/\Delta A_{dye}(\lambda_{dye})$ was determined from difference spectra of the dye titration. λ_{dye} is the absorption maximum of the dye, i.e., 590 nm for BCP and 570 nm for CR. From the maximal amplitude of the corrected depletion signal $\Delta A_{corr}(\lambda,t)$ and the dye signal at infinite dye concentration $\Delta A(\lambda_{dye},f \rightarrow \infty)$ [given by the product of the fit parameters p and $\Delta A(1)$] the number of protons per cycling molecule was calculated:

$$n = \frac{\Delta A(\lambda_{dye},f \rightarrow \infty)/\epsilon_{dye}(\lambda_{dye})}{\Delta A_{corr}(\lambda,t)/\epsilon_{PYP}(\lambda)} \qquad (3)$$

This requires knowledge of the extinction coefficients of the protein ϵ_{PYP} and the dye ϵ_{dye} at the respective wavelengths.

Spectral and Kinetic Analysis. The dye signals of the unbuffered and the buffered samples were analyzed using the assumption that the same spectral components occur in both datasets but with different time traces. Thus a singular value decomposition (SVD) of the joint array of buffered and unbuffered data was performed (*34*):

$$(\Delta\mathbf{A}_u, \Delta\mathbf{A}_b) = \mathbf{U}^T\mathbf{D}(s)(\mathbf{V}_u, \mathbf{V}_b) \qquad (4)$$

The subscripts u and b refer to the unbuffered and the buffered measurements, respectively. In this way the basis spectra (columns of $\mathbf{U}^T$) of both datasets $\Delta\mathbf{A}_u$ and $\Delta\mathbf{A}_b$ are the same, while different contributions $\mathbf{V}_u$ and $\mathbf{V}_b$ arise which represent the kinetic evolution for the two measurements. A linear transformation $\mathbf{X}$ provides the absorbance spectra $\mathbf{A}$ and the concentration changes $\Delta\mathbf{n}$ of the physically relevant species ("true states") involved:

$$\mathbf{A} = \mathbf{U}^T\mathbf{X}^{-1} \quad \text{and} \quad (\Delta\mathbf{n}_u, \Delta\mathbf{n}_b) = \mathbf{X}\mathbf{D}(s)(\mathbf{V}_u, \mathbf{V}_b) \qquad (5)$$

The transformation is not unique, but the constraint that the spectrum of one of the true states should represent the dye in solution reduces this ambiguity. The remaining parameters were chosen in compliance with subjective criteria on the shape of the spectra and the time traces.

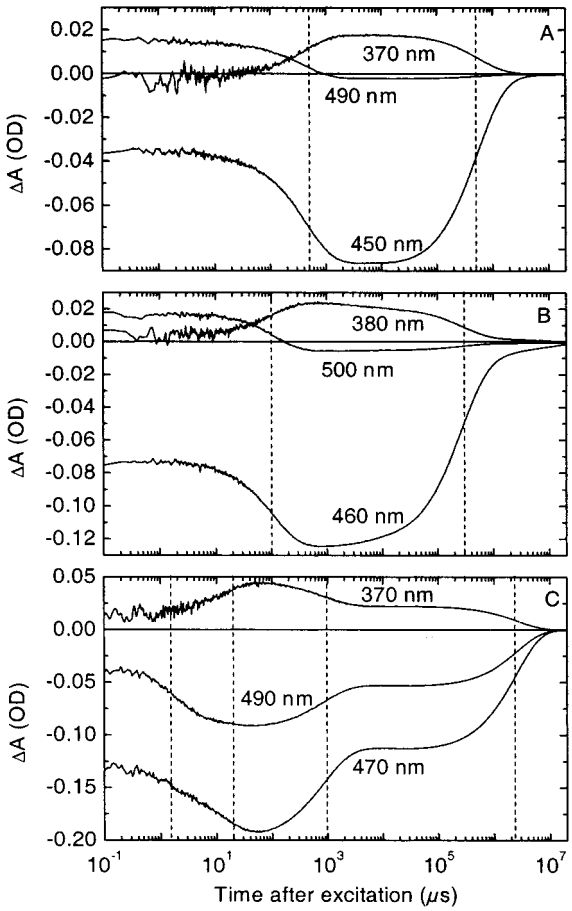

FIGURE 1: Transient absorbance changes $\Delta A(t)$ of unbuffered solutions of PYP at three wavelengths as indicated. Panels: (A) wild type, pH 6.3; (B) E46Q, pH 6.3; (C) E46A, pH 8.3. Dashed vertical lines mark the time constants of the main components in the rise and the decay of I_2.

RESULTS

Photocycles of Wild Type, E46Q, and E46A. The flash-induced transient absorbance changes of wild type and the mutants E46Q and E46A were measured at a large number of wavelengths. Typical results at selected wavelengths are presented in Figure 1. Please note the logarithmic time scale. Panel A shows data for wild type at wavelengths of 490, 370, and 450 nm, which are diagnostic for the red-shifted I_1 intermediate, the blue-shifted I_2 intermediate, and the depletion signal of P (446 nm), respectively. From the decay of the signals at 490 and 450 nm and the simultaneous rise of the absorbance at 370 nm, we conclude that the I_1 to I_2 transition occurs in several hundred microseconds. From the decay of the signals at 370 and 450 nm we conclude that the system returns from I_2 to the initial dark state P in several hundred milliseconds at pH 6.3. All measurements in Figure 1 were performed at 20 °C and 50 mM KCl in the absence of buffer, with excitation at 430 nm for wild type and the mutant E46Q and at 440 nm for the mutant E46A. The corresponding traces for the mutant E46Q, also at pH 6.3, are shown in panel B. This mutant has its absorption maximum in P at 460 nm, and correspondingly somewhat higher values were chosen for the measuring wavelengths

selected for I_1 (500 nm), I_2 (380 nm), and P (460 nm) than in wild type. The overall pattern in panel B is the same as in panel A, but there are several important differences. An I_2-like intermediate is clearly formed in this mutant but with a considerably shorter rise time of about 100 μs. Moreover, the return to P has a second very slow component of several seconds. Panel C shows the time traces for the mutant E46A at 370, 490, and 470 nm. In this mutant the p*K* of the chromophore protonation in the dark is 7.9 (*32*). Above this p*K*, in the yellow alkaline form, the chromophore is deprotonated with its absorbance maximum at 465 nm (*32*). The data of panel C were therefore taken at pH 8.3 with excitation at 440 nm. Under these pH and excitation conditions the percentage of molecules with protonated chromophores (acidic form with absorption maximum at 365 nm) that contributes to the transient absorbance signal was estimated from the absorption spectrum and from the titration curve to be less than 2%. This estimate is supported experimentally by the fact that excitation at the lower wavelength of 430 nm, i.e., at a wavelength at which more molecules in the acidic form could be excited, had no significant effect on the photocycle kinetics. Selective excitation of the population of molecules with deprotonated chromophores was thus achieved by a combination of the choice of pH and excitation wavelength. The trace at 370 nm shows that also in E46A an I_2-like intermediate with a protonated chromophore is formed. The traces at 370, 470, and 490 nm show that in this mutant the formation of I_2 is even faster, occurring with times of about 2 and 20 μs. The return to P is biphasic with a fast time of about 1 ms and a slow time of several seconds, separated by a long plateau. The trace at 370 nm shows that after the fast phase an equilibrium is reached between intermediates with protonated (I_2) and deprotonated chromophores.

Comparison of Proton Uptake/Release Kinetics with Chromophore Protonation/Deprotonation Kinetics. The kinetics of proton uptake and release by PYP from the aqueous medium was measured at pH 6.2 with the pH-indicator dye bromocresol purple and at pH 8.3 with the dye cresol red as explained in Materials and Methods. In panel A of Figure 2 the kinetics of proton transfer with the aqueous medium, as monitored by the absorbance signal at 590 nm (top; absorption maximum of the deprotonated dye), is compared with the photocycle kinetics as monitored by the depletion signal at 450 nm (bottom) for wild type at pH 6.2. The traces at 590 nm (dye) and 450 nm (chromophore) were fitted simultaneously with a sum of exponentials. An adequate fit required four exponentials, two associated with the rise of I_2 and a transition between two I_2-like intermediates and two associated with the decay of I_2. No systematic deviations occurred as evidenced by the residuals (not shown). The arrows mark the values of the four common exponential time constants. The kinetic constants obtained from the fits to the data of Figure 2 are collected in Table 1. The fact that both the photocycle and dye signals can be fitted well with the same set of time constants is strong evidence that the kinetics of chromophore protonation/deprotonation (ΔA at 370 nm) and the kinetics of proton uptake/release by PYP (ΔA at 590 nm) are perfectly synchronized.

Our data indicate that the amplitude of the millisecond component (τ_2) is larger in the dye signal than in the depletion signal. Recent FTIR experiments also detected two components in the rise of I_2 with similar times as observed here optically (*13*, *21*). Moreover, these vibrational data provided evidence for the nature of the molecular events associated with the times of 500 μs and 4.8 ms observed here for the rise of I_2 (*21*). The first time was assigned to the protonation of the chromophore, and the second time was attributed to a major conformational change between two I_2 states (i.e., intermediates with protonated chromo-

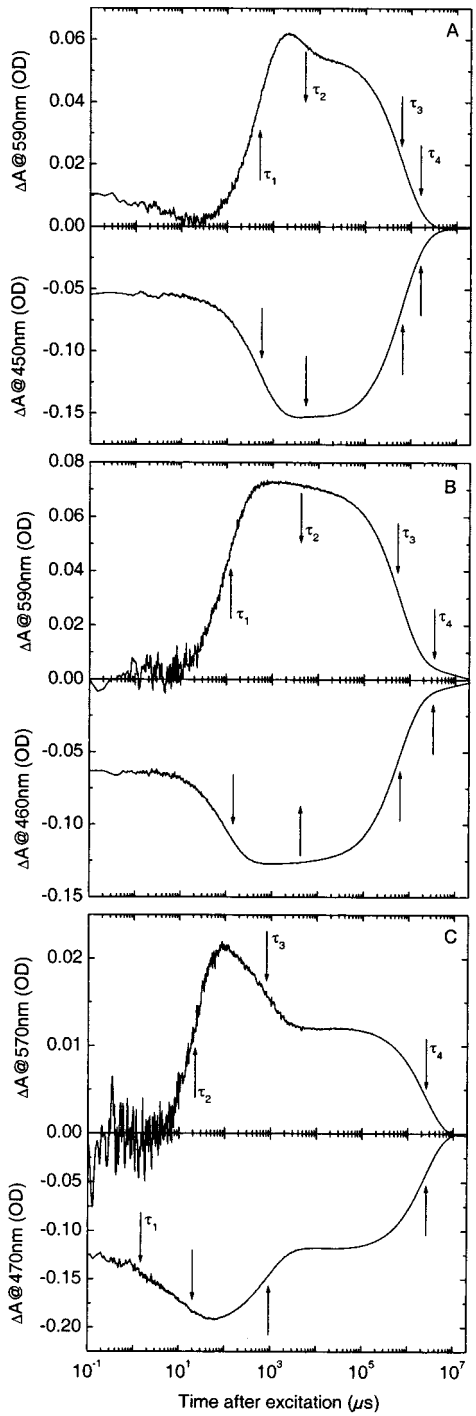

FIGURE 2: Transient absorbance changes $\Delta A(t)$ of unbuffered solutions of PYP and of pH-indicator dyes at the respective λ_{max}. The arrows indicate the time constants of a simultaneous fit of the two time traces. Panels: (A) wild type, pH 6.2, bromocresol purple, $\tau_1 = 500$ μs, $\tau_2 = 4.8$ ms, $\tau_3 = 600$ ms, $\tau_4 = 1.8$ s; (B) E46Q, pH 6.2, bromocresol purple, $\tau_1 = 110$ μs, $\tau_2 = 4.1$ ms, $\tau_3 = 550$ ms, $\tau_4 = 3.2$ s; (C) E46A, pH 8.3, cresol red, $\tau_1 = 1.6$ μs, $\tau_2 = 20$ μs, $\tau_3 = 870$ μs, $\tau_4 = 2.4$ s.

Table 1: Simultaneous Fit of Photocycle Kinetics and pH-Indicator Kinetics of PYP[a]

sample	pH	τ_1	τ_2	τ_3	τ_4
wild type	6.2	500 μs	4.8 ms	600 ms	1.8 s
E46Q	6.2	110 μs	4.1 ms	550 ms	3.2 s
E46A	8.3	1.6 μs	20 μs	870 μs	2.4 s

[a] Excitation at 430 nm for wild type and E46Q and at 440 nm for E46A. Data of Figure 2.

phores). In the next section we will present evidence that confirms the FTIR interpretation of the slower millisecond transition as a structural change in which the protonated state of the chromophore does not change. The data in panel A thus show that formation of a protonated chromophore with simultaneous uptake of a proton from the aqueous medium occurs around 500 μs after flash excitation. With considerable delay this is followed by a transition to another protein state with protonated chromophore in about 4 ms. Biphasic deprotonation of the chromophore and decay to P occur with times of 600 ms and 1.8 s, which are precisely mirrored by two corresponding phases in the proton release to the external medium.

The corresponding data for the mutant E46Q, again at pH 6.2, are shown in panel B of Figure 2. Formation of I_2 (chromophore protonation; bottom) and proton uptake (top) are again perfectly synchronized in this mutant with a rise time that is accelerated to 110 μs. The conformational transition at 4.1 ms has a smaller amplitude but occurs with about the same time constant as in wild type. Chromophore deprotonation and proton release are also closely kinetically coupled. This includes the very long tail with 3.2 s that is present in both signals. Except for some changes in the values of the time constants and amplitudes, the tight kinetic coupling between chromophore protonation/deprotonation and proton uptake/release observed for wild type is preserved in this mutant. We note that E46Q lacks the putative internal proton donor E46.

Panel C shows the data for the yellow alkaline form of the mutant E46A. As we saw in the previous section, an I_2-like intermediate with a deprotonated chromophore is formed in this mutant (trace at 370 nm in Figure 1C), and its kinetics is reflected in the depletion signal at 470 nm. The measurements were performed at pH 8.3 with excitation at 440 nm to select only the alkaline form. At this pH we used the dye cresol red. Its deprotonated form has an absorption maximum at 570 nm, and accordingly ΔA at this wavelength is shown in the top panel of Figure 2C. A simultaneous fit of both the dye and depletion signals was again possible, as indicated with four exponential time constants as marked by the arrows. Formation of I_2 is accelerated even further in E46A with time constants of 1.6 and 20 μs. The amplitude of the 1.6 μs component in the depletion signal is about half that of the main 20 μs component. Due to the high pH of 8.3 the ratio of the transient dye signal to the depletion signal is smaller for this mutant than for wild type and E46Q, which were measured at pH 6.2. The signal-to-noise ratio of the dye signal in the submicrosecond time domain is moreover lower than in panels A and B where the dye signal occurred later and was larger. It remains therefore uncertain whether the dye signal also contains the 1.6 μs component with significant amplitude. Chromophore protonation and proton uptake are however both accelerated with respect to wild type and E46Q and remain concerted. The chromophore deprotonation occurs in two phases (870 μs and 2.4 s) as is also evident from the 370 nm trace in Figure 1C. As we will see in the next section, the 870 μs phase is clearly accompanied by proton release and is not due to a conformational change. We conclude that after 870 μs an equilibrium is reached between an I_2 state and an intermediate with a deprotonated chromophore. We further note that proton release at 870 μs and 2.4 s is exactly mirrored by chromophore deprotonation. As in wild type and E46Q, the chromophore protonation/deprotonation reactions in E46A are perfectly coupled to proton uptake/release.

Wavelength Heterogeneity in Dye Kinetics Is Due to Transient Dye Binding. The dye kinetics in the absence of buffer were measured not just at 590 nm, the absorption maximum of its deprotonated form, but at 12 wavelengths from 520 to 630 nm in steps of 10 nm. Surprisingly, the kinetics were clearly wavelength dependent, suggesting inhomogeneity due to the presence of more than one species/component. This is illustrated in panel A of Figure 3 where only the traces at the two wavelengths 590 and 620 nm are shown. The 620 nm trace was scaled to match the latter part (>30 ms) of the 590 nm trace (dotted trace). The wavelength dependence of the kinetics is apparent. If the dye signal is entirely due to transient protonation changes, it should completely disappear in the presence of buffer. Panel B shows however that in the presence of a saturating concentration of 10 mM sodium phosphate buffer a substantial residual signal of about 3−4 m OD remains. At 590 nm the amplitude of this nonproton signal is negative; at 620 nm, positive. Subtracting this buffer-resistant part of the signal (panel B) from the signal in the absence of buffer (panel A) leads to the true protonation signal shown in panel C. After this correction the time traces in panel C have the same kinetics and can be scaled simultaneously at all times. This is demonstrated in panel C where the 620 nm trace was scaled to the 590 nm trace (dottted trace). Within experimental error the two traces match. This is not just true at the two wavelengths shown but at all 12 wavelengths. The dye signals in the absence and presence of buffer at all 12 wavelengths were analyzed by SVD and fitted simultaneously with a sum of exponentials leading to the three exponential time constants of 540 μs, 3.2 ms, and 690 ms, which are indicated by the common vertical dashed lines. Note that the dye signal which is not due to protons (panel B) rises with the slow 3.2 ms time and does not contain a significant contribution from the fast 540 μs component. The large 3.2 ms component in the dye signal of panel A has almost entirely disappeared after the correction (panel C). This suggests that PYP takes up a proton with $\tau = 540$ μs, remains protonated for several decades, and releases a proton with $\tau = 690$ ms. In panel D the amplitude of the true protonation signal (panel C) after 2 ms (approximate maximum) is plotted against the observation wavelength (solid squares) and compared with the scaled difference spectrum of the free deprotonated minus protonated dye (solid line). The agreement is excellent, indicating that the corrected transient proton signal of panel C is indeed due to transient deprotonation of the dye and transient proton uptake by PYP.

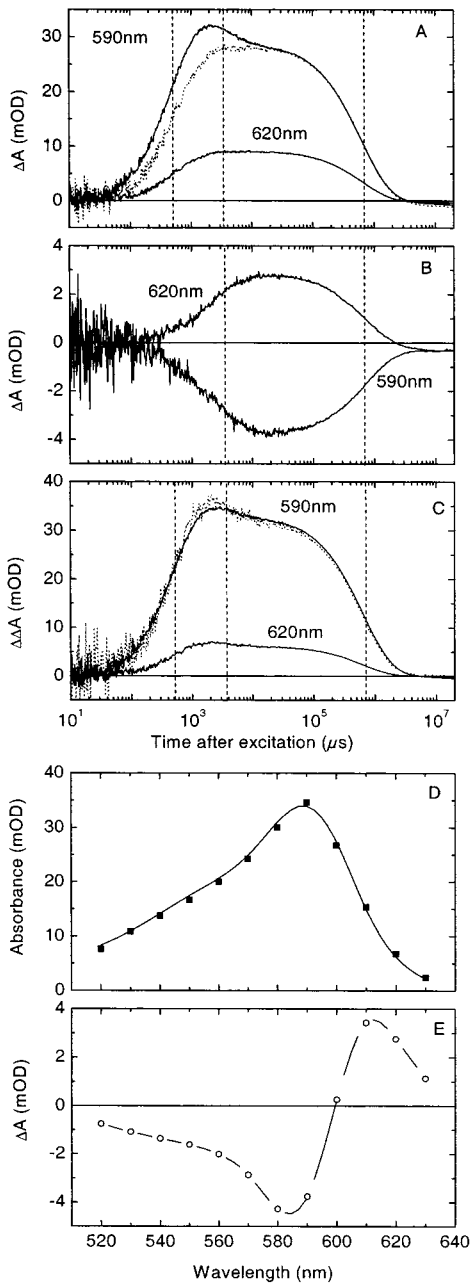

FIGURE 3: Transient dye signal (bromocresol purple) obtained with wild-type PYP, pH 6.2. (A, B, C) Time traces at the indicated wavelengths (solid lines) and scaled signal at 620 nm (dotted lines): (A) unbuffered, (B) 10 mM sodium phosphate, and (C) difference of (A) and (B). Vertical dashed lines label the time constants of the involved transitions: $\tau_1 = 540$ μs, $\tau_2 = 3.2$ ms, $\tau_3 = 690$ ms. (D) Wavelength dependence of the absorbance difference at 2 ms in (C) (solid squares) and pH-induced difference spectrum of bromocresol purple (solid line). (E) Wavelength dependence of the buffered dye signal of (B) at 20 ms.

We turn now to the interpretation of the nonproton component in the dye absorbance change which rises with 3.2 ms (panel B). The sign of ΔA is negative below about 595 nm and positive above. The complete wavelength dependence of ΔA at 20 ms after flash excitation (approximately the maximal value) is shown in panel E. This difference spectrum is typically what one would expect for a red shift of the BCP spectrum with an isosbestic point between 595 and 600 nm. This strongly suggests that this buffer-resistant component is due to transient binding of the dye to a hydrophobic region of the protein in I_2. This explanation is supported by transient dye deprotonation data at various molar dye to PYP ratios. With increasing dye concentration (10, 20, 30, 40 μM) the amplitude of the binding contribution to the total dye signal increased (data not shown). This is consistent with a shift of the equilibrium between free PYP and PYP with bound dye. The amplitude of the binding contribution ΔA in the presence of buffer also increased 3-fold with increasing pH from 5.8 to 6.6 (data not shown). Remembering that only the deprotonated form of the dye contributes at 590 nm, this effect can also be understood on the basis of transient dye binding. Increasing the pH leads to more deprotonated dye with a corresponding increase in the concentration of the dye−protein complex. In conclusion, we have strong evidence that the millisecond component in the dye signal is due to transient binding of the dye to a new state of PYP with a protonated chromophore which we call I_2'. In agreement with FTIR results (*21*) this conformational change in I_2 occurs several milliseconds after excitation and about one decade in time after proton uptake.

The corresponding dye data for the mutant E46Q at two wavelengths in the absence and presence of saturating amounts of buffer are shown in panels A and B, respectively, of Figure 4. The wavelength dependence of the dye signal is evident from panel A. After correction for dye binding, the time traces at all wavelengths have the same shape. This is demonstrated in panel C, where the scaled 620 nm trace (dotted line) fits well with the 590 nm trace. A simultaneous fit of the dye signals in the absence and presence of buffer at the 12 wavelengths led to the three time constants of 110 μs, 4 ms, and 1 s indicated by the vertical dashed lines. The transient dye binding signal (panel B) rises with $\tau = 4$ ms, about the same value as for wild type. Its relative amplitude (compared to the unbuffered dye signal) is smaller than in wild type, which suggests a smaller conformational change. The corrected true protonation signal (panel C) now contains only the two time constants indicated, suggesting that protonation of PYP occurs around 110 μs after the flash with no further protonation change until the return to P. Panel D shows that the amplitude of the true protonation signal (solid squares) exactly matches the difference spectrum (solid line) of the deprotonated free dye.

Similar experiments were performed with the mutant E46A in the form with a deprotonated chromophore in the initial dark state. In panel A of Figure 5 time traces of the dye signal (cresol red, pH 8.3) are shown at the four wavelengths 530, 550, 570, and 590 nm in the absence of buffer. The shape of these traces is the same for every wavelength. In contrast to wild type and E46Q, there is no wavelength dependence for this mutant. Moreover, consistent with this observation, the signal at 570 nm disappears completely in the presence of 10 mM Tris (panel A). We conclude that in this mutant no transient dye binding occurs. Simultaneous fitting of the four traces in panel A led to the three time constants 20 μs, 870 μs, and 2.4 s marked by the dashed vertical lines. The fastest time of 20 μs corresponds to proton uptake. In this mutant probably no conformational change occurs on the milisecond time scale. Instead, a partial proton release occurs at 870 μs, leading to an equilibrium between I_2 and a state with a deprotonated chromophore. In panel B the amplitude of the dye signal at the four wavelengths, 100 μs after the flash (solid squares), is compared with the scaled pH-induced difference spectrum (deprotonated minus pro-

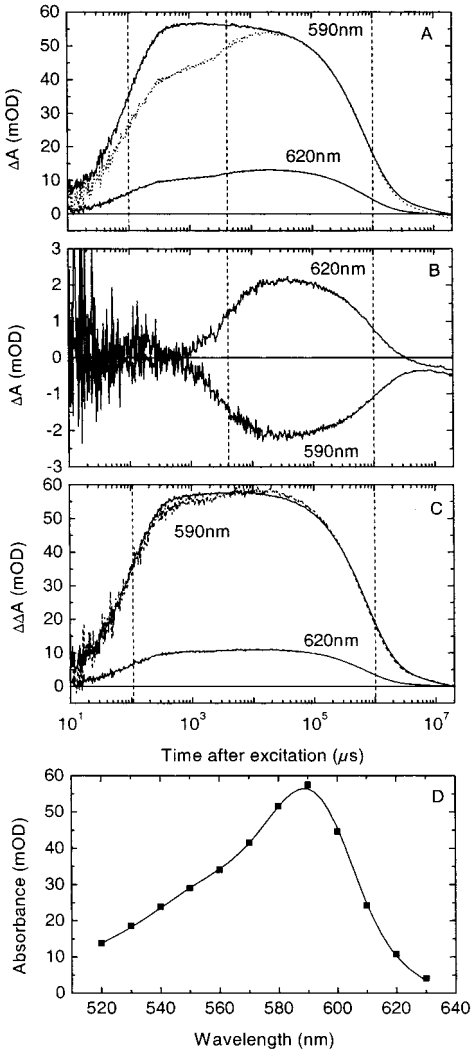

FIGURE 4: Transient dye signal (bromocresol purple) obtained with the mutant E46Q, pH 6.2. (A, B, C) Time traces at the indicated wavelengths (solid lines) and scaled signal at 620 nm (dotted lines): (A) unbuffered, (B) 10 mM sodium phosphate, and (C) difference of (A) and (B). Vertical dashed lines label the time constants of the involved transitions: $\tau_1 = 110$ μs, $\tau_2 = 4.1$ ms, $\tau_3 \sim 1$ s. (D) Wavelength dependence of the absorbance difference at 3 ms in (C) (solid squares) and pH-induced difference spectrum of bromocresol purple (solid line).

tonated) of cresol red (solid line). Again, the agreement is excellent.

Singular Value Decomposition Analysis of the Dye Kinetics. Further evidence for the coexistence of free and bound deprotonated dye populations was obtained from a quantitative SVD analysis of the transient absorption data of the dye. A joint SVD analysis of the dye signals for the unbuffered and buffered (pH 6.2) state of the same sample at all 12 measuring wavelengths was performed as described in Materials and Methods. The resulting singular values s_i are plotted on a logarithmic scale in panel A of Figure 6. There are clearly two dominating values, $s_1 = 1.019$ and $s_2 = 0.105$, which are above the noise level as indicated by the dashed line. In the following we therefore only considered these main contributions. The two basis spectra $U_{s\lambda}$ are shown in panel B and are orthogonal as required. The corresponding time traces V_{st} are displayed in panel C. There are two time traces for the unbuffered state of the sample (labeled s_1^u and s_2^u) and two for the buffered state (labeled s_1^b, s_2^b). The four

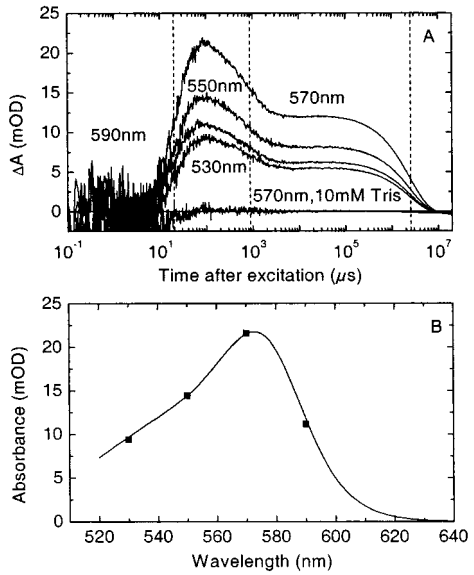

FIGURE 5: Transient dye signal (cresol red) obtained with the mutant E46A, pH 8.3. (A) Time traces at the indicated wavelengths, unbuffered except for the lower 570 nm trace which is in the presence of 10 mM Tris. The dashed vertical lines mark the exponential time constants of the transitions: $\tau_1 = 20$ μs, $\tau_2 = 870$ μs, $\tau_3 = 2.4$ s. (B) Wavelength dependence of the absorbance difference at $\sim$100 μs in (A) (solid squares) and pH-induced difference spectrum of cresol red (solid line).

weighted time traces sV_{st} were fitted simultaneously with a sum of exponentials. Using three exponentials the corresponding exponential time constants were 540 μs, 3.2 ms, and 690 ms. Four exponentials provided an excellent fit with time constants 540 μs, 3.0 ms, 600 ms, and 1.9 s. The residuals are shown in panels D (for the s_1 traces) and E (for the s_2 traces). The first time constants of 540 μs and 3.0 ms are compatible with the results from Figure 2 (500 μs, 4.8 ms). A different sample was used here, possibly with a somewhat different pH. Moreover, in Figure 2 two photocycle and dye traces were analyzed at two wavelengths, whereas in Figure 6 only dye data but under different conditions (*u*nbuffered, *b*uffered) were analyzed simultaneously at 12 wavelengths.

As described in Materials and Methods the basis spectra $U_{s\lambda}$ and time traces V_{st} were transformed by the 2×2 matrix **X** into component absorption spectra $A_{i\lambda}$ and corresponding concentration changes $\Delta n_i(t)$. Two of the matrix elements of **X** were determined by requiring that the absorption spectrum of one of the components equals the deprotonated minus protonated difference spectrum of the free dye. The other two matrix elements of **X** were fixed by the experimental observation that the absorption spectrum of the second component should be red shifted and by the requirement that the time traces $\Delta n_i(t)$ should have the expected signs. The results of this analysis are shown in Figure 7. The spectrum labeled D_1 (solid squares) is the spectrum of the first component corresponding to the free unprotonated dye. This spectrum matches almost perfectly the measured difference spectrum (solid line). D_2 is the spectrum of the bound deprotonated dye. It is clearly red shifted by approximately the amount estimated from the data of Figure 3. The resulting concentration changes are shown in the lower panel. D_1^u labels the time course of the first component (free deprotonated dye) in the unbuffered state. The concentration rises

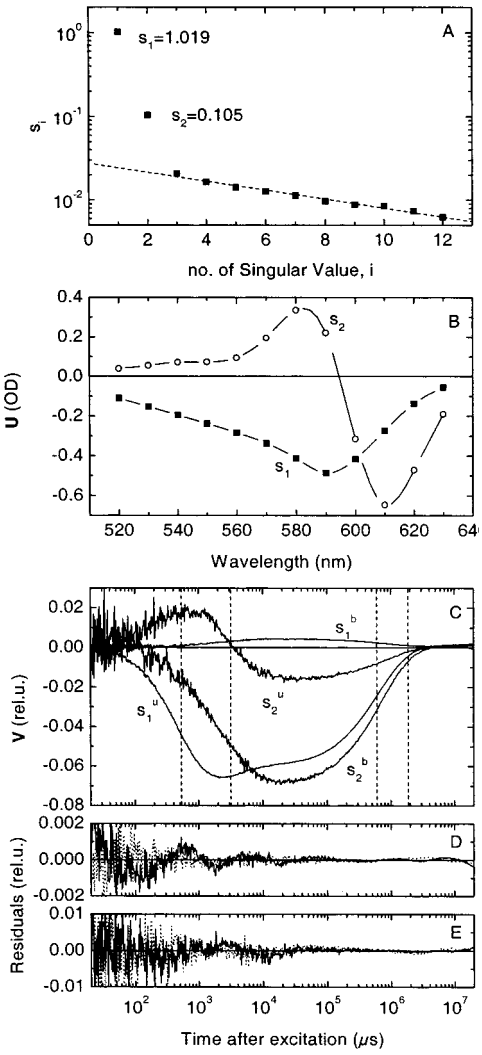

FIGURE 6: SVD analysis of the joint data array of the unbuffered and the buffered dye signals for wild-type PYP, pH 6.2. Panels: (A) singular values; (B) basis spectra; (C) time traces. Superscripts u and b label the unbuffered and the buffered traces, respectively. (D) Residuals of a simultaneous fit with four exponentials to the four time traces of (C), weighted with the respective singular values. Shown in (D) are the residuals for the traces labeled s_1^u and s_1^b in (C). (E) Residuals of the traces labeled s_2^u and s_2^b in (C). Time constants of the common fit with four exponentials: $\tau_1 = 540$ μs, $\tau_2 = 3.0$ ms, $\tau_3 = 600$ ms, $\tau_4 = 1.9$ s.

with $\tau \approx 500$ μs and then partially decays with $\tau \approx 3$ ms. Concomitantly with this decay the concentration of the second component labeled D_2^u (bound deprotonated dye) rises. D_1^b and D_2^b label the corresponding time courses for the buffered state of the sample. These traces do not contain a significant 500 μs component, since the protons are buffered away. With the slow 3 ms time constant the concentration of the free deprotonated dye is depleted (D_1^b, negative Δn), whereas simultaneously the concentration of the bound deprotonated dye increases (D_2^b). The fact that the traces of D_2^u and D_2^b are nearly the same is not dependent on the choice of the variable elements of **X**, indicating that the dye binding is not affected by the buffer.

The results of the SVD analysis thus strongly support the more qualitative analysis of the previous section. First, it shows that two linearly independent components are required. Second, it shows that, by an appropriate choice of the matrix elements of **X**, a self-consistent analysis of the data is

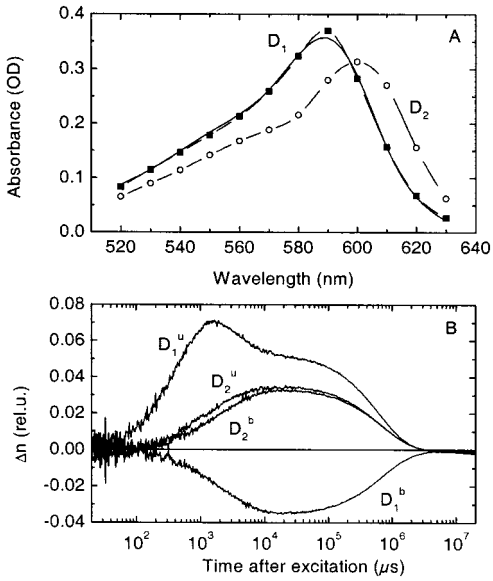

FIGURE 7: Linear transformation of the SVD basis spectra and time traces of Figure 6B,C for wild-type PYP. (A) Spectra (■, ○). The continuous curve that matches the D_1 data points is the scaled measured difference spectrum between the free deprotonated and protonated forms of the dye. The D_2 spectrum represents the bound form of the deprotonated dye. (B) Time traces of the relative concentration changes. The subscript refers to the two different dye species. The superscripts u and b refer to the unbuffered and buffered conditions.

possible in terms of two components. The spectra and time courses of these components show that a red-shifted bound dye component rises with $\tau \approx 3$ ms for both the buffered and unbuffered states of the sample.

Proton Uptake Stoichiometry. The stoichiometry of proton uptake or release is usually determined by calibrating the dye signal by microtitration and normalizing to the concentration of photoreceptor molecules that cycle (*35*). In many cases this calibration procedure is not very accurate, since the addition of concentrated acid or base often leads to local aggregation or denaturation which in turn causes errors in ΔA. For these reasons we employed a different method which does not require this calibration procedure. Instead, we measured the transient dye absorbance signal as a function of the dye concentration at fixed PYP concentration. With increasing dye concentration the absorbance change saturates since ultimately every proton is detected. Equation 1 of Materials and Methods describes the dependence of the dye signal on the dye concentration. A fit of the data to this equation yields the two parameters p and $\Delta A(1)$, allowing the calculation of the dye signal at infinite dye concentration ($\Delta A(f \rightarrow \infty) = p\Delta A(1)$). Using this value the stoichiometry is then calculated from eq 3 of Materials and Methods, which requires in addition the concentration of PYP molecules that cycle. The latter is determined from the depletion signal (ΔA at λ_{max}). The procedure is demonstrated in Figure 8 for the mutant E46Q at pH 6.3. In panel A the dye signal at 590 nm is shown at the four dye concentrations of 10, 20, 30, and 40 μM. The PYP concentration was 9 μM. The depletion signal at 460 nm also depended on the dye concentration. This is due to two effects. First, the dye also absorbs at 460 nm so that the depletion signal contains a small transient dye component that is linear in the dye concentration. This could be easily corrected using the spectral titration data of

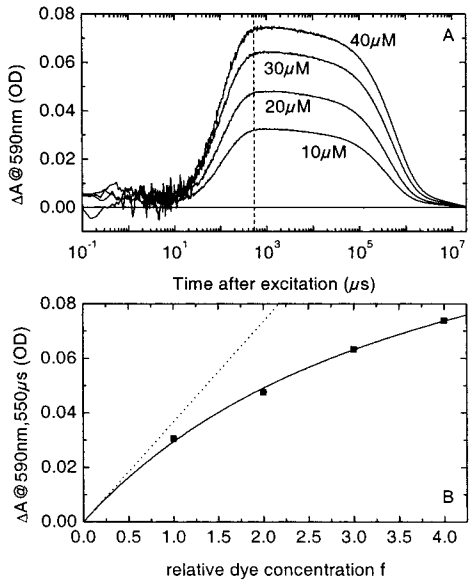

FIGURE 8: Light-induced transient absorbance changes at 590 nm of a sample of E46Q (concentration 9 μM, pH 6.3) at four different concentrations (*f*) of the pH-indicator dye bromocresol purple. (A) Time traces (the dashed vertical line marks 550 μs). (B) Dye signal at 550 μs (solid squares) versus relative dye concentration f = [dye]/10 μM. The solid line is a fit to the data with eq 1. The dotted line indicates the predicted dependence in the absence of saturation effects.

the dye as explained in Materials and Methods (eq 2). The second effect is due to the fact that with increasing dye absorbance at 460 nm fewer PYP molecules were excited. After correction for the transient dye contribution the depletion signal at 460 nm was therefore normalized to the same maximal value by applying a scaling factor. This same scaling factor was applied to obtain the dye signals at 590 nm shown in Figure 8A. The maximal amplitudes at 550 μs (vertical dashed line) are clearly nonlinear in the dye concentration. These ΔA values at 550 μs are plotted in Figure 8B as a function of the relative dye concentration *f*, defined as the dye concentration in units of 10 μM. The dye signal shows clear saturation behavior. The straight line through the origin indicates the linear signal increase expected in the absence of saturation. The continuous curve through the data points is the best fit to eq 1. From the good quality of the fit we conclude that the data can indeed be described by eq 1. The corresponding fit parameters are $p = 5.02$ and $\Delta A(1) = 0.029$ OD. The amplitude of the depletion signal at 460 nm was $\Delta A = 0.113$ OD. Using the extinction coefficients $\epsilon_{590} = 50000\ M^{-1}\ cm^{-1}$ for the dye BCP and $\epsilon_{460} = 45500\ M^{-1}\ cm^{-1}$ for the E46Q mutant, the stoichiometry was calculated from eq 3 to be 1.2. Similar data were collected for wild type and the mutant E46A (data not shown). Analyzing these in the same way, a stoichiometry of 0.8 was obtained for wild type.

With E46A the data were collected at pH 8.3. At this high pH and due to the fact that only a fraction of the molecules were in the yellow alkaline form, the measurements with E46A had to be performed at a higher protein concentration of 25 μM to achieve a reasonable proton signal. As a consequence the data points at the dye concentrations from 10 to 40 μM were in the linear range, and no reliable stoichiometry could be determined. Instead, we used a different procedure for this mutant, first described in ref *31*. In this method the stoichiometry is obtained from an analysis of the dependence of the signal on the buffer concentration, at fixed concentrations of protein and dye. The dye signal was measured at Tris concentrations of 15, 50, 100, 200, 1000, and 10 000 μM. The decrease in the dye signal with increasing buffer concentrations was analyzed as in ref *31*. In this way we obtained a stoichiometry of 0.7 for the mutant E46A. We note that our analysis assumes that the molecules in the acid form of E46A are not excited and that the extinction coefficient of the basic form of E46A equals that of wild type.

DISCUSSION

In this study we investigated the kinetic coupling between proton uptake by PYP and chromophore protonation. The goal was to contribute to the question of what the source of the protons is that protonates the chromophore. Since FTIR studies show that deprotonation of E46 and protonation of the chromophore are synchronized, it seems reasonable to believe that the chromophore is deprotonated directly by the internal donor E46 to which it is hydrogen bonded in the initial dark state (*13*, *21*). The synchronization is not sufficient proof in itself, however, since concurrently with chromophore isomerization and rotation the proton of E46 could be transferred to some neighboring group X^-. Using pH-indicator dyes, it was observed that proton uptake by PYP and chromophore protonation are synchronized, suggesting that the chromophore is protonated from the aqueous medium (*14*). This view is supported by structural data which show that the phenolate oxygen is close to the protein surface in I_2 (*14*). In itself this evidence is not conclusive either: the conformational change in I_2 could lead to p*K* changes of surface groups with concomitant proton uptake. Recent FTIR results indicate however that deprotonation of E46 and protonation of the chromophore occur with the early rise time of I_2 of 260 μs (*21*), whereas the global conformational change is clearly delayed with $\tau \approx 2$ ms (*21*). If the protons that are taken up were Bohr protons associated with the structural change, they should also appear with the slower millisecond time. As we have shown here, they are always associated with the fastest time in the formation of I_2.

When E46 was replaced by glutamine, the formation of I_2 was significantly accelerated (*6*). Since glutamine can still form a hydrogen bond but is unable to transfer a proton, this observation does not fit in with the role of E46 as internal donor. To explain this without invoking protonation from the external medium, a group XH was postulated which takes over from E46 and is more efficient than E46 in its absence (*21*).

Here we have used time-resolved absorption spectroscopy to monitor both the kinetics of chromophore protonation (absorption increase at 370 nm and decrease at 450 nm) and the kinetics of proton uptake (ΔA of dye at 590 nm). In wild type we find from a simultaneous fit of photocycle and dye data that proton uptake is perfectly synchronized with the formation of I_2 (about 500 μs at pH 6.2). In the mutant E46Q both I_2 formation and proton uptake are accelerated to about 100 μs (pH 6.2) but remain kinetically coupled. In the alkaline form of the mutant E46A we find that an I_2-like intermediate is formed (chromophore protonation) and that formation of this I_2 is further accelerated (two rise times of

1.6 and 20 μs) with a concurrent acceleration of proton uptake. We note that no significant 1.6 μs component was detected in the dye signal which was also quite noisy in this early time range (see Figure 2C). This may be due to the limited intrinsic time resolution of CR which is determined by its rate constant for deprotonation (*36*). In wild type and E46Q the stoichiometry of proton uptake was close to 1. Whereas these data are perfectly consistent with protonation from the aqueous medium in all three systems, they cannot be explained by internal protonation from E46 unless some very special assumptions are invoked. An alternative internal donor XH would be required, for example, which would be a better donor than E46 in the absence of this group in the mutants E46Q and E46A. We therefore conclude that the simplest explanation of all the data, chromophore protonation from the aqueous medium, should at present be the preferred explanation.

A second conclusion from our work is that the dye bromocresol purple binds transiently to an I_2 state of PYP. Thus this dye binding signal is a useful kinetic indicator to monitor the structural transition from I_2 to I_2'. This conclusion is based on the observation that in the presence of excess buffer a transient dye absorption change remains which is not due to dye deprotonation. This effect was analyzed in detail using the dependence of this dye binding signal on wavelength, pH, and dye concentration. The existence of two independent components in the transient dye signal was quantitatively established using a combined SVD analysis of the data in the absence and presence of buffer. The two SVD basis spectra $U_{s\lambda}$ and time traces V_{st} could be transformed into two-component spectra and the corresponding component time courses. The spectrum of the bound deprotonated dye was red shifted by the appropriate amount, whereas the time courses were in excellent agreement with the more qualitative analysis based on subtracting the dye signals in the presence of buffer from those in the absence of buffer. In wild type the dye binding occurs at pH 6.2 with a time constant of about 3.2 ms. This is clearly much delayed with respect to proton uptake ($\tau = 500$ μs). These results are in excellent agreement with recent FTIR measurements which indicate that the conformational change occurs 2.0 ms [pH 7 (*21*)] or 1.5 ms [pH 7.0 (*13*)] after the flash. We have thus confirmed the timing of this structural change using an independent method. As in ref *21* we assume that I_2' is on a sequential pathway between I_2 and the initial state P. This is the simplest model consistent with our data. Further work is required to prove this photocycle model.

This conformational change is often described as a partial unfolding (*16*) in which a hydrophobic patch is exposed to the solvent. It is not surprising that a dye such as bromocresol purple can bind to such a site. We confirmed that lower dielectric media such as methanol induce a red shift in the spectrum of the deprotonated form of bromocresol purple (data not shown). It is also well-known that BCP binds to bovine serum albumin (BSA) with a substantial red shift and that the change in the BCP spectrum upon binding can be used to estimate the amount of BSA (*37*). Titrating the anionic form of BCP with BSA, the isosbestic point is at 598 nm, close to our estimated value of between 595 and 600 nm. Moreover, the measured difference spectrum when BCP binds to BSA (*37*) has a striking quantitative similarity with panel E of Figure 3, and the absolute spectra of the free and bound forms correspond closely to the D_1 and D_2 spectra from our SVD analysis (Figure 7A) (*37*). The results of the extensive measurements on BCP binding to BSA (see also references in ref *37*) fully support our interpretation of the nonproton part of the transient dye signal as binding to the I_2 form of PYP. We could not detect any change in the spectrum of BCP when PYP was added in the dark. In view of the large spectral effect with BSA, we conclude that no binding occurs in the dark state of PYP. Our measurements also clearly show that the chromophore remains protonated when the conformational change occurs in wild type and E46Q. The transition is thus between two I_2 states which we call I_2 and I_2'.

It is interesting that, in previous work with the dye BCP and PYP at pH 6.0 in 50 mM MES buffer and 1 M KCl, no transient dye binding was said to be observed (*23*). However, upon closer examination of their Figure 1B, a difference spectrum with crossover around 600 nm may be discerned that has the same shape as our difference spectrum of Figure 3E. Moreover, the ratio of the amplitude of this bound dye signal to the signal amplitude in the absence of buffer is also about what we observed. We conclude that the authors overlooked this evidence for transient dye binding in their data. This may have been due to the insensitive way they plotted the data or to the small signal-to-noise ratio.

Whereas in wild type the time constants for proton uptake and conformational change are 540 μs and 3.2 ms, respectively, these times are 110 μs and 4.1 ms in the mutant E46Q (both at pH 6.2). Proton uptake is clearly accelerated in E46Q, but the timing of the conformational change is barely affected. Our data further indicate that the dye binding signal is smaller in E46Q, suggesting a smaller structural change. This is in agreement with FTIR data which indicated smaller amplitudes for the difference spectra in the amide I band in this time range (*21*).

With the mutant E46A we had to work at the higher pH of 8.3 to be sure we were selecting the yellow alkaline form with an excitation wavelength of 440 nm. Accordingly, we had to use another dye, cresol red, with an appropriate p*K*. In contrast to the results with wild type and E46Q, the dye signal with E46A was entirely due to protons, and no dye binding was detected. The simplest explanation is that no conformational change occurred. However, we cannot entirely exclude that the absence of dye binding was due to the different nature of the dye or to the higher pH. We note however that we also performed dye measurements with cresol red at pH 8.3 on wild type and that transient dye binding was observed (data not shown). The apparent decrease in the amplitude of the conformational change from wild type to E46Q and to E46A may now be rationalized as follows. In wild type the breakage of the electrostatic and hydrogen-bonding interactions with E46 and Y42 when the chromophore rotates out of the binding pocket leads to a structural reorganization in the binding pocket in which E46 and Y42 find new interaction partners. With considerable delay this local structural change relaxes and develops into a global structural change. In E46Q the interaction of Q46 with the chromophore in the dark is weaker, leading to a smaller structural change. Finally, in E46A there is no interaction of A46 with the chromophore, and no reorganization occurs.

For the mutant E46A we established with measurements at 370 and 470 nm that an I_2-like intermediate with a protonated chromophore is formed. In previous studies a fast time and slow time in the decay of the depletion signal were noted (*32*). Here we confirm this finding and show moreover that these two time constants in the depletion signal are exactly mirrored in the decay of I_2 at 370 nm and in the proton release signal. The fast time thus represents the partial transition to a state with a deprotonated chromophore and the simultaneous release of protons. The simplest interpretation of these findings using a sequential photocycle model is that an equilibrium is established between I_2 and a state with a deprotonated chromophore that relaxes to P with the slow decay time (see Figures 2C and 1C).

The slower (>10 ns) part of the photocycle of PYP and its mutants has not yet been investigated in great detail except in ref *10*. For wild type most authors describe the formation of I_2 with one exponential time constant and the return from I_2 to P with another exponential time constant. In ref *9* formation of I_2 occurs with two time constants of ≈200 μs and 5 ms. The return to P occurs with a time constant of about 600 ms. In ref *10* both the rise and decay of I_2 are biexponential. For the rise of I_2 these authors obtained time constants of 250 μs and 1.2 ms with relative amplitudes of 60% and 40%, respectively, at pH 7.5 and 19 °C. Thus our time constants of 500 μs and 4.8 ms at pH 6.2 and 20 °C (Table 1) are compatible with the previous work. For the recovery of the ground state values of 150 ms and 2.0 s were obtained in ref *10*, comparable with our values of 600 ms and 1.8 s (Table 1). Few data are available for the mutants E46Q and E46A. For E46Q at neutral pH, single exponential time constants were obtained for the rise and the decay of I_2 of about 50 μs and 50 ms (*6*). In our experiment at pH 6.2 we obtained two exponential time constants for the rise of I_2 (110 μs and 4.1 ms, Table 1) and two for the decay (550 ms and 3.2 s, Table 1). Since these time constants are strongly pH dependent and due to the difference in the number of observed components, our data are consistent with the previous work. For E46A the rise of I_2 in the alkaline form is resolved here for the first time. For the biphasic decay of I_2 we obtained time constants of 870 μs and 2.4 s at pH 8.3, which should be compared with 125 μs and 2 s at pH 8.0 in the previous work (*32*).

We note that in all cases proton release is perfectly coupled to the decay of I_2. This is also in agreement with a tight coupling between the protonation changes of the chromophore and the aqueous medium.

To determine the proton stoichiometry, we developed a novel extrapolation method which is very simple and does not require the inaccurate calibration procedure. It is based on the fact that with increasing dye concentration the dye signal due to protons will saturate since ultimately every proton will be detected. The experimental data obeyed the analytical form of eq 1. The method requires some saturation which can only be reached at high molar dye to PYP ratios. Since for E46A these conditions could not be reached, a different procedure was applied in this case. For wild type, E46Q, and E46A, the proton stoichiometry is close to 1, consistent with the binding of a single proton to the exposed phenolic oxyanion of the chromophore.

APPENDIX

Saturation of the Absorption Change of the Deprotonated Dye with the Dye Concentration. We assume that the protein and the dye act as competing buffers:

$$X^- + H^+ \rightleftharpoons XH \text{ (dye)} \quad \text{and} \quad Y^- + H^+ \rightleftharpoons YH \text{ (protein)}$$

The dependence of the concentrations of the species X^- and Y^- on the pH is given by the Henderson−Hasselbalch equation. For small pH changes this equation may be linearized, and the relation is substantially simplified:

$$\Delta[X^-](f) = fC_X\Delta\text{pH}(f) \tag{A1}$$

$$\Delta[Y^-](f) = C_Y\Delta\text{pH}(f) \tag{A2}$$

C_X and C_Y are constants.The factor f expresses the fact that the concentration change of the deprotonated dye species is proportional to the dye concentration f for a given pH change ΔpH. This pH change depends in turn on the protonation change $\Delta[H^+]$ (the concentration change due to proton uptake or proton release by PYP), on the concentration change of the deprotonated dye species, and on the concentration change of Y^-:

$$\Delta[H^+] = -\Delta[X^-](f) - \Delta[Y^-](f) - C_Z\Delta\text{pH}(f) \tag{A3}$$

Equation A3 is a proton balance or conservation equation. The protons taken up or released by PYP (left) must be balanced by the sum of all the protonation changes of the dye, the protein, and water (right). Therefore, the pH change depends on the dye concentration f. From these three equations (A1−A3) the pH change ΔpH(f) and $\Delta[Y^-](f)$ can be eliminated and we get

$$\Delta[H^+] = -\left(1 + \frac{C_Y + C_Z}{C_X f}\right)\Delta[X^-](f) \tag{A4}$$

Replacing $(C_Y + C_Z)/C_X$ by C_A and rearranging eq A4 yields

$$\Delta[X^-](f) = -\Delta[H^+]\frac{1}{1 + C_A/f} \tag{A5}$$

This equation shows that the concentration change of X^- as a function of f depends on only two independent parameters, $\Delta[H^+]$ and C_A.

For a more convenient representation we consider $\Delta[X^-](1) = -\Delta[H^+]/(1 + C_A)$ and introduce the new parameters $\Delta[X^-](1)$ and $p = 1 + C_A$ instead of $\Delta[H^+]$ and C_A:

$$\Delta[X^-](f) = \Delta[X^-](1)\frac{f}{1 + (f-1)/p} \tag{A6}$$

Multiplying eq A6 on both sides by the extinction coefficient ϵ_{dye} of the deprotonated dye and the sample thickness d, we get the following hyperbolic dependence of the observed absorbance change $\Delta A(f)$ on f with $\Delta A(1)$ and p as parameters:

$$\Delta A(f) = \Delta A(1)\frac{f}{1 + (f-1)/p} \tag{A7}$$

REFERENCES

1. Meyer, T. E. (1985) *Biochim. Biophys. Acta 806*, 175−183.

2. Sprenger, W. W., Hoff, W. D., Armitage, J. P., and Hellingwerf, K. J. (1993) *J. Bacteriol. 175*, 3096−3104.
3. Pellequer, J.-L., Wager-Smith, K. A., Kay, S. A., and Getzoff, E. D. (1998) *Proc. Natl. Acad. Sci. U.S.A. 95*, 5884−5890.
4. Kim, M., Mathies, R. A., Hoff, W. D., and Hellingwerf, K. J. (1995) *Biochemistry 34*, 12669−12672.
5. Borgstahl, G. E. O., Williams, D. R., and Getzoff, E. D. (1995) *Biochemistry 34*, 6278−6287.
6. Genick, U. K., Devanathan, S., Meyer, T. E., Canestrelli, I. L., Williams, E., Cusanovich, M. A., Tollin, G., and Getzoff, E. D. (1997) *Biochemistry 36*, 8−14.
7. Kort, R., Vonk, H., Hoff, W. D., Crielaard, W., and Hellingwerf, K. J. (1996) *FEBS Lett. 382*, 73−78.
8. Unno, M., Kumauchi, M., Sasaki, J., Tokunaga, F., and Yamauchi, S. (2000) *J. Am. Chem. Soc. 122*, 4233−4234.
9. Meyer, T. E., Yakali, E., Cusanovich, M. A., and Tollin, G. (1987) *Biochemistry 26*, 418−423.
10. Hoff, W. D., Van Stokkum, I. H. M., Van Ramesdonk, H. J., Van Brederode, M. E., Brouwer, A. M., Fitch, J. C., Meyer, T. E., Van Grondelle, R., and Hellingwerf, K. J. (1994) *Biophys. J. 67*, 1691−1705.
11. Ujj, L., Devanathan, S., Meyer, T. E., Cusanovich, M. A., Tollin, G. and Atkinson, G. H. (1998) *Biophys. J. 75*, 406−412.
12. Genick, U. K., Soltis, S. M., Kuhn, P., Canestrelli, I. L., and Getzoff, E. D. (1998) *Nature 392*, 206−209.
13. Brudler, R., Rammelsberg, R., Woo, T. T., Getzoff, E. D., and Gerwert, K. (2001*) Nat. Struct. Biol. 8*, 265−270.
14. Genick, U. K., Borgstahl, G. E. O., Ng, K., Ren, Z., Pradewand, C., Burke, P. M., Srajer, V., Teng, T. Y., Schildkamp, W., McRee, D. E., Moffat, K., and Getzoff, E. D. (1997) *Science 275*, 1471−1475.
15. Imamoto, Y., Mihara, K., Hisatomi, O., Kataoka, M., Tokunaga, F., Bojkova, N., and Yoshihara, K. (1997) *J. Biol. Chem. 272*, 12905−12908.
16. Van Brederode, M. E., Hoff, W. D., Van Stokkum, I. H. M., Groot, M.-L., and Hellingwerf, K. J. (1996) *Biophys. J. 71*, 365−380.
17. Rubinstenn, G., Vuister, G. W., Mulder, F. A. A., Düx, P. E., Boelens, R., Hellingwerf, K. J., and Kaptein, R. (1998) *Nat. Struct. Biol. 5*, 568−570.
18. Hoff, W. D., Xie, A., Van Stokkum, I. H. M., Tang, X., Gural, J., Kroon, A. R., and Hellingwerf, K. J. (1999) *Biochemistry 38*, 1009−1017.
19. Meyer, T. E., Tollin, G., Hazzard, J. H., and Cusanovich, M. A. (1989) *Biophys. J. 56*, 559−564.
20. Ren, Z., Perman, B., Srajer, V., Teng, T.-Y., Pradervand, C., Bourgeois, D., Schotte, F., Ursby, T., Kort, R., Wulff, M., and Moffat, K. (2001) *Biochemistry 40*, 13788−13801.
21. Xie, A., Kelemen, L., Hendriks, J., White, B. J., Hellingwerf, K. J. and Hoff, W. D. (2001) *Biochemistry 40*, 1510−1517.
22. Meyer, T. E., Cusanovich, M. A., and Tollin, G. (1993) *Arch. Biochem. Biophys. 306*, 515−517.
23. Hendriks, J., Hoff, W. D., Crielaard, W., and Hellingwerf, K. J. (1999) *J. Biol. Chem. 274*, 17655−17660.
24. Emeis, D., Kuhn, H., Reichert, J., and Hofmann, K. P. (1982) *FEBS Lett. 143*, 29−34.
25. Parkes, J. H., and Liebman, P. A. (1984) *Biochemistry 23*, 5054−5061.
26. Dickopf, S., Mielke, T., and Heyn, M. P. (1998) *Biochemistry 37*, 16888−16897.
27. Olson, K. D., Deval, P., and Spudich, J. L. (1992) *Photochem. Photobiol. 56*, 1181−1187.
28. Tokutomi, S., Yamamoto, K. T., Miyoshi, Y., and Furuya, M. (1982) *Photochem. Photobiol. 35*, 431−433.
29. Van Thor, J., Borucki, B., Crielaard, W., Otto, H., Lamparter, T., Hughes, J., Hellingwerf, K. J., and Heyn, M. P. (2001) *Biochemistry 40*, 11460−11471.
30. Otto, H., Marti, T., Holz, M., Mogi, T., Lindau, M., Khorana, H. G., and Heyn, M. P. (1989) *Proc. Natl. Acad. Sci. U.S.A. 86*, 9228−9232.
31. Grzesiek, S., and Dencher, N. A. (1986) *FEBS Lett. 208*, 337−342.
32. Devanathan, S., Brudler, R., Hessling, B., Woo, T. T., Gerwert, K., Getzoff, E. D., Cusanovich, M. A., and Tollin, G. (1999) *Biochemistry 38*, 13766−13772.
33. Borucki, B., Otto, H., and Heyn, M. P. (1999) *J. Phys. Chem. B 103*, 6371−6383.
34. Henry, E. R., and Hofrichter, J. (1992) *Methods Enzymol. 210*, 129−192.
35. Otto, H., Marti, T., Holz, M., Mogi, T., Stern, L. J., Engel, F., Khorana, H. G., and Heyn, M. P. (1990) *Proc. Natl. Acad. Sci. U.S.A. 87*, 1018−1022.
36. Gutman, M., and Nachliel, E. (1990) *Biochim. Biophys. Acta 1015*, 391−414.
37. Nakamaru, Y., and Sato, C. (1997) *Biochim. Biophys. Acta 1341*, 207−216.

BI0256227